Iranian Journal of Microbiology

Volume 17 Number 6 (December 2025) 977-990
DOI: http://doi.org/10.18502/ijm.v17i6.20366

ORIGINAL ARTICLE

Yeast-mediated display: probing *Helicobacter pylori* HopQ and CEACAM1 interaction

Nasim Mofarrah, Mohaddeseh Larypoor*, Jamileh Norozi

Department of Microbiology, Faculty of Biological Science, North Tehran Branch, Islamic Azad University, Tehran, Iran

Received: March 2025**, Accepted:** August 2025

ABSTRACT

Background and Objectives: *Helicobacter pylori (H. pylori)*, as a Gram-negative pathogen plays a key role in causing gastritis, peptic ulcer disease, and gastric malignancies. The bacterial adhesin HopQ binds human CEACAM1, promoting adherence and CagA oncoprotein translocation. This study aimed to establish a yeast-based surface expression platform to investigate the HopQ–CEACAM1 interaction as a basis for future inhibitor screening.
Materials and Methods: The N-terminal domain of human CEACAM1 (C1ND) was displayed on the surface of *Saccharomyces cerevisiae* BY4741 as C1ND or C1ND–EGFP via Aga2 fusion. Constructs were introduced by electroporation and confirmed by PCR. Protein expression and localization were validated by western blot, confocal microscopy, and flow cytometry. Binding assays involved GFP-tagged HopQ and GFP-expressing *H. pylori.*
Results: Western blot confirmed surface expression of C1ND and C1ND–EGFP. Confocal microscopy and flow cytometry showed strong fluorescence signals, with significantly higher mean fluorescence intensity and anti-GFP–positive yeast compared to controls ($P < 0.01$). Yeast-displayed C1ND specifically bound HopQ–GFP and GFP-expressing *H. pylori.*
Conclusion: Yeast surface display of CEACAM1's N-domain is an effective model for studying HopQ–CEACAM1 binding and offers potential for identifying inhibitors to block *H. pylori* adhesion and associated disorders.

Keywords: *Helicobacter pylori*; HopQ; CEACAM1; C1ND

INTRODUCTION

Helicobacter pylori is a microaerophilic Gram-negative microorganism colonizing nearly half of humankind, with prevalence varying widely by geographic location—for example, it is significantly higher in developing regions (1, 2). Colonization by *H. pylori* represents a major etiological determinant of gastritis, peptic ulcer disease, and gastric cancer (3, 4). The cytotoxin-associated gene A (CagA) encodes an oncoprotein that is translocated into host gastric cells through a type IV secretion apparatus (5, 6). Once inside host cells, CagA undergoes tyrosine phosphorylation at several conserved EPIYA segments, enabling interaction with cellular target proteins (7, 8). These interactions disrupt the regulation of homeostatic signaling in gastric epithelial tissues, promoting persistent inflammation and malignant transformation (9, 10).

In addition, the outer membrane proteins (OMPs) of *H. pylori* are essential for the bacterium's attachment and colonization of human gastric epithelial cells (11). Among these, HopZ, BabA, SabA, OipA, and HopQ contributes significantly to *H. pylori* ad-

*Corresponding author: Mohaddeseh Larypoor, Ph.D, Department of Microbiology, Faculty of Biological Science, North Tehran Branch, Islamic Azad University, Tehran, Iran. Tel: +98-9122885346 Fax: +98-77009848 Email: M.larypoor@iau.ir

herence and disease induction (3, 12, 13). HopQ itself is an OMP of *H. pylori* (14, 15), and exists in two allelic variants, type I and type II, which share approximately 70% amino acid sequence identity (15). HopQ mediates bacterial attachment to gastric epithelia by engaging CEACAM receptors (16, 17).

CEACAMs (carcinoembryonic antigen-related cell adhesion molecules) are glycoproteins belonging to the immunoglobulin superfamily and the CEA family. They are expressed on cell surfaces and function as cell adhesion molecules (18, 19). Carcinoembryonic antigen-related cell adhesion molecule 1 (CEACAM1), also known as carcinoembryonic antigen-related cell adhesion molecule 1, is pivotal in mediating cellular attachment, growth regulation, and immune modulation (20, 21). Additionally, CEACAM1 participates in vascular development, tumor advancement, and metastatic spread (22). CEACAM1, along with CEACAM5 and CEACAM6, shows elevated expression during *H. pylori*–associated gastritis and gastric carcinoma, whereas their expression levels are much lower in a healthy stomach (23). In *H. pylori*, HopQ selectively binds the N-terminal IgV domain of CEACAM1 and also recognizes CEACAM3, 5, and 6 (23, 24). The interaction between HopQ and CEACAMs is essential for facilitating the translocation of CagA into gastric epithelial cells. (16, 17).

The N-terminal IgV-like domain of CEACAM1 (C1ND) functions as the main interface for ligand binding (18, 25). Type I HopQ binds to C1ND via an induced-fit mechanism (24), specifically engaging residues 1-108 of C1ND (23, 24). Yeast or bacterial surface-display systems enable peptide or protein presentation on the cell exterior (26, 27). Among these microorganisms, *Saccharomyces cerevisiae* (*S. cerevisiae*) is non-pathogenic and possesses a eukaryotic glycosylation system for secreted proteins. Compared to bacteria and phages, *S. cerevisiae* enables the surface display of larger and more complex proteins (28, 29). The α-agglutinin system from *S. cerevisiae* is widely used for stable surface display of proteins (29). α-agglutinin, a GPI-anchored protein, comprises two subunits: Aga1, which is anchored in the yeast cell wall, and Aga2, which can be fused to a target protein and binds to Aga1 via disulfide linkages (30).

In the present work, we employed a yeast surface-display platform to present the C1ND domain fused with the Aga2 component of α-agglutinin on the surface of *S. cerevisiae*. We then investigated and visualized the interaction between surface-displayed C1ND and HopQ-GFP using confocal microscopy, as well as the interaction between surface-displayed C1ND and *H. pylori* expressing recombinant GFP. This engineered yeast system provides a proof-of-concept platform for studying the C1ND-HopQ interaction, which could support future screening efforts.

Therefore, this work sought to design and confirm the functionality of a yeast-based display system expressing the N-terminal domain of CEACAM1 (C1ND) to assess its specific binding to *H. pylori* HopQ as a proof-of-concept platform. As far as we are aware, this work represents the first demonstration of expressing the N-terminal IgV-like domain (C1ND) of human CEACAM1 on the surface of *S. cerevisiae* using a yeast surface display system. This novel approach establishes a unique platform for investigating the HopQ-CEACAM1 interaction.

MATERIALS AND METHODS

Bacteria and yeast strains and culture conditions. For plasmid transformations in this study, *Escherichia coli* strain TOP10F' was used. *E. coli* strains were maintained in Luria–Bertani (LB) medium under standard growth conditions (containing yeast extract, sodium chloride, peptone, and distilled water) at 37°C overnight with agitation at 150 rpm. Transformed *E. coli* colonies were plated on Luria–Bertani agar containing ampicillin (100 µg/mL) and incubated overnight at 37°C.

S. cerevisiae strain BY4741 was used for the yeast transformation via electroporation with recombinant plasmids and for displaying fusion proteins on the cell surface. *S. cerevisiae* cultures were grown in YPD broth (1% yeast extract, 2% peptone, and 2% dextrose) with orbital agitation at 200 rpm and incubated at 29°C overnight. Following electroporation, transformed yeast cells were cultured in synthetic defined CAA (SD-CAA) medium containing glucose, yeast nitrogen base, casamino acids, and phosphate salts, and monosodium phosphate) and incubated at 30°C (31). It should be noted that *Saccharomyces boulardii* was used solely as a positive technical control in this study. The strain expressing Aga2-EGFP-PL1 was derived from a separate project in our laboratory and was not part of the main experimental objectives or scientific investigation of this work.

Construction of DNA plasmids for surface display in *S. cerevisiae*. A surface display plasmid, designated pYES2-Tef1-display-C1ND (Fig. 1), was constructed. The coding sequence for the N-terminal IgV-like domain of CEACAM1 (C1ND), consisting of 324 base pairs (bp) and encoding 108 amino acids (~12 kDa), was amplified by PCR using primers C1ND-F and C1ND-R with human genomic DNA as the template. To facilitate cloning, XhoI restriction sites and a His-tag were incorporated at the 5′ end of the gene, and an XbaI restriction site was added at the 3′ end during primer design.

The PCR-amplified C1ND fragment was digested with XhoI and XbaI restriction endonucleases and subsequently cloned into the pre-constructed pYES2-Tef1 expression vector. This vector contains the Tef1 promoter, which drives the expression of Aga2 fusion proteins, such as C1ND or C-myc-EGFP-G4S-C1ND. The resulting construct was designated pYES2-Tef1-display-C1ND.

For the construction of the EGFP fusion, the EGFP gene was amplified by PCR with XhoI restriction sites at both ends. The amplified fragment was digested with XhoI and inserted into the XhoI restriction site of pYES2-Tef1-display-C1ND, resulting in the construction of the recombinant plasmid pYES2-Tef1-display-GFP-C1ND.

Each cloning step was verified by DNA sequencing to confirm accuracy. Primers for amplifying the C1ND gene fragment were designed using SnapGene software and synthesized by SinaClone; their sequences are enumerated in Table 1. Additional primers available in the laboratory are listed in Table 2 (32).

Transformation of recombinant plasmids into yeast. Each plasmid (pYES2-Tef1-display-C1ND and pYES2-Tef1-display-GFP-C1ND) was independently transferred into *S. cerevisiae* BY4741 via electroporation.

First, An isolated BY4741 colony was introduced into 5 mL of YPD medium and cultivated at 29°C under agitation (250 rpm) for approximately 16 h. The overnight culture was diluted into 50 mL fresh YPD and further incubated until reaching mid-log phase ($OD_{600} \approx 0.4–0.8$).

Cells were collected by centrifuging at 4,000 rpm for 5 min at 5°C, rinsed twice with sterile water, and once with 1 M sorbitol.

For electroporation, 50 µl of prepared yeast cells were mixed with 5 µl of plasmid DNA, and pulsed using the Gene Pulser Xcell™ (Bio-Rad Laboratories, USA) with parameters of 1.5 kV, 200 Ω, and 25 µF. Transformed cells were transferred into SD-CAA medium and incubated at 30°C for up to three days (33).

PCR confirmation of transformed colonies. To verify the presence of pYES2-Tef1-display-C1ND and pYES2-Tef1-display-GFP-C1ND plasmids in the transformed *S. cerevisiae* colonies, multiple colonies were randomly selected and screened by PCR. The primers TEF1-F, AGA2-F, C1ND-F, C1ND-R, EGFP-F, and EGFP-R were used for amplification. Col-

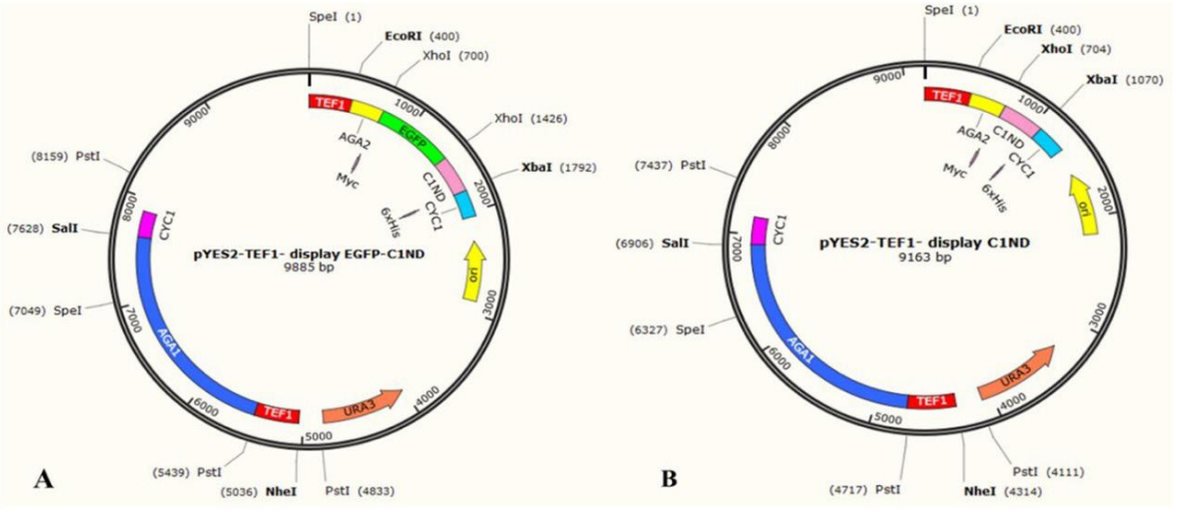

Fig. 1. Diagram showing the pYES2-derived expression constructs designed to produce the fusion proteins AGA1–AGA2–c-Myc–EGFP–G4S–C1ND (A) and AGA1–AGA2–c-Myc–G4S–C1ND (B) in *S. cerevisiae.*

Table 1. Primer design. Sequences in bold indicate restriction enzyme recognition sites and His-tag sequence.

Primers	Sequences (5'–3')	Length of the gene fragment	Tm (°C)
C1ND-F	CCGCTCGAGGGTGGTGGAGGCTCTCAGCTCACTACTG	324 bp	78.3
C1ND-R	TGCTCTAGATTAATGATGATGATGATGATGCGGGTATAC	324 bp	68.4

Table 2. Primers available in the laboratory. Bolder sequences indicate restriction enzyme recognition sites.

Primers	Sequences (5'–3') GCTAGCATAGCTTCAAAATG
TEF1-F	TGAATTCAAAACAATGCAGTTACTTCGCTGTT
AGA2-F	CCGCTCGAGGACCCGGTGAGCAAGGGCGAGGA
EGFP-F	CCGCTCGAGCTTGTACAGCTCGTCCATGC
EGFP-R	

onies showing the expected PCR products were considered positive transformants and were subsequently isolated for further analysis (31).

Evaluation of target protein expression by immunoblotting. To verify the expression of the recombinant Aga2–C-myc–EGFP–G4S–C1ND construct, yeast transformants were grown in 5 mL YNB medium containing 0.5 g L^{-1} casamino acids, 2 g L^{-1} glucose, and 0.17 g L^{-1} yeast nitrogen base (with ammonium sulfate, amino acid–free) at 30°C, 200 rpm, for 72 h.

Cells were pelleted by centrifugation (3,000 rpm, 5 min) and resuspended in lysis buffer containing 25 mM Tris–HCl, 250 mM sucrose, 10 mM EDTA, 1 mM PMSF, and 1 mM DTT (33). DTT was added to detach the Aga2–C-myc–EGFP–G4S–C1ND fusion from the yeast surface. Surface proteins were obtained by mild sonication using a mixture of yeast cells, buffer, and glass beads (1:2:1); samples were vortexed for 3 min in six cycles with 2-min cooling on ice between steps.

The cell wall–associated supernatant was obtained by centrifuging at 10,000 rpm for 1 min and was then subjected to 12% SDS–PAGE analysis. Supernatant from *S. cerevisiae* harboring pYES2-Tef1-display-GFP-C1ND served as the positive control, while untransformed *S. cerevisiae* strain BY4741 served as the negative control.

Following SDS–PAGE, resolved proteins were electroblotted onto nitrocellulose membranes (Thermo Scientific, USA) using 300 mA current for 1 h. Blots were incubated overnight at 4°C in TBST containing 1% (w/v) skim milk for blocking nonspecific binding.

Immunoblots were probed overnight at 4°C with HRP-labeled antibodies against GFP (1:2000; Acris, USA), His-tag (1:1000; Sigma, USA), and C1ND (1:3000; Sigma, USA). After antibody incubation, membranes were rinsed four times (5 min each) in TBST.

Protein bands were visualized using either enhanced chemiluminescence (ECL) reagent or DAB staining with the HRP Chromogenic Substrate Kit (Sigma-Aldrich, USA).

Flow cytometric analysis. Positive *S. cerevisiae* transformants were cultured for 72 hours in 10 ml of YNB medium containing 0.67% yeast nitrogen base (ammonium sulfate, amino acid–free) supplemented with 2% sucrose or galactose (Sigma-Aldrich, USA), and incubated at 30°C under agitation (200 rpm).

Cells were collected by centrifugation and rinsed twice with sterile PBS. After washing, PE-conjugated anti-GFP antibody (2.5 µg/ml) was added to a suspension of 5×10^2 cells, and samples were kept in the dark at 4°C for 1 h to allow antibody binding.

For negative control assays, *S. cerevisiae* carrying the empty pYES2 vector was treated identically using 2.5 µg/mL PE-labeled anti-GFP antibody (per 5×10^2 cells) and incubated at 4°C for 1 h in darkness to establish baseline fluorescence.

Following incubation, After incubation, unbound antibodies were removed by three washes with ice-cold PBS, and cells were finally resuspended in 700 µL PBS supplemented with 1 mg/mL BSA (34).

Samples were analyzed using a BD FACSCalibur flow cytometer (BD Biosciences, San Jose, CA, USA). Flow cytometry data, including mean fluorescence intensity (MFI) measurements, were analyzed using FlowJo software (Tree Star, Inc., San Carlos, CA, USA).

Confocal microscopy. Yeast cells expressing the Aga2–C-myc–EGFP–G4S–C1ND recombinant construct on their surface were cultured in YNB medium as described previously until reaching an OD_{600} of 1.0, then pelleted by centrifugation (4,000 rpm, 5 min).

Cells were washed once in phosphate-buffered saline (PBS) and resuspended (~10^2 cells) in 700 µL PBS supplemented with 1 mg/mL BSA. The suspension was incubated with 2.5 µl stained with PE-labeled anti-GFP antibody (BioLegend, USA) for 2 h at ambient temperature.

Following incubation, cells underwent three consecutive washes with PBS supplemented with 1 mg/mL BSA to remove unbound antibodies. A drop of the final suspension was placed on a microscope slide for imaging using an LSM800 confocal microscope (Carl Zeiss, Germany).

Unmodified *S. cerevisiae* strain BY4741 served as the negative control strain.

Analysis of the interaction between yeast surface-displayed C1ND and HopQ-GFP. Yeast cells expressing surface-displayed C1ND were incubated with HopQ-GFP protein (2.5 mg/ml) at ratios of 1:10 and 1:100 incubated for 1 h under ambient temperature conditions. After incubation, cells were pelleted by centrifugation, rinsed with PBS, and preserved in 4% paraformaldehyde (35). Following fixation, cells were again centrifuged, rinsed with PBS, and stained for 20 min in 3 µM DAPI. The samples were then examined using fluorescence and confocal microscopy. The unmodified BY4741 strain was used as the negative control (36).

Specificity controls for C1ND-HopQ binding assays. For assessing binding specificity, yeast cells expressing AGA2-C1ND without EGFP were incubated with HOPQ-GFP. After washing, fixation, and DAPI staining, samples were analyzed by confocal microscopy.

In the blocking assay, yeast displaying AGA2-C1ND was pre-incubated with anti-C1ND antibody before exposure to HOPQ-GFP. Samples were then washed, fixed, stained, and examined under confocal microscopy.

As a negative control, yeast expressing AGA2-C1ND without EGFP was incubated with AGA2-GFP protein. Following washing, fixation, and DAPI staining, cells were analyzed by confocal microscopy.

Analysis of the interaction between yeast surface-displayed C1ND and *H. pylori* expressing EGFP. Yeast cells expressing the recombinant Aga2–C-myc–EGFP–G4S–C1ND construct were cultured in YNB medium as previously described.

Concurrently, *H. pylori* strain TN2 expressing GFP was cultured on Brucella Blood Agar for 72 hours. A single bacterial colony was then transferred to liquid BHI medium and incubated under microaerophilic conditions cultivated at 37°C under agitation until the optical density (OD_{600}) reached 2.0.

The yeast culture was centrifuged to collect the yeast cells. Varying amounts of yeast (10^6, 10^9, and 10^{12} cells) pellets were resuspended in 1 mL BHI broth containing *H. pylori* TN2 and co-incubated for 2 h at room temperature to enable interaction.

After incubation, the samples were centrifuged, washed two times with PBS and treated with 4% paraformaldehyde for 15 min at room temperature to fix the cells. DAPI staining followed the procedure described earlier. Fluorescence and confocal microscopy (LSM800; Carl Zeiss, Germany) were used to visualize the yeast–bacterium complexes.

Non-transformed *S. cerevisiae* strain BY4741 was included served as the negative control strain.

Statistical investigation. All statistical evaluations were carried out in GraphPad Prism version 8 (GraphPad Software, USA). Normality of the data was verified using the Shapiro–Wilk test. For normally distributed datasets, group comparisons of mean fluorescence intensity (MFI) were made using Welch's t-test. Differences with $P < 0.05$ were regarded as statistically significant.

RESULTS

Construction of recombinant *S. cerevisiae* expressing surface-displayed C1ND. Recombinant plasmids pYES2-Tef1-display-C1ND and pYES2-Tef1-display-GFP-C1ND were generated and introduced into *S. cerevisiae* BY4741 through electropo-

ration. Fig. 1 illustrates the expression cassettes and their components.

To verify the correct transformation of the target plasmids into yeast, colony PCR was performed on *S. cerevisiae* transformants. Using primers GFP-F/GFP-R and AGA2-F/C1ND-R for the plasmid pYES2-Tef1-display-GFP-C1ND, the expected bands at 700 bp and 1,346 bp were detected (Fig. 2, lanes 1 and 2). PCR with primers AGA2-F/C1ND-R and TEF1-F/C1ND-R for the plasmid pYES2-Tef1-display-C1ND (without the GFP tag) resulted in amplified fragments of 646 bp and 1,069 bp, respectively (Fig. 2, lanes 3 and 4). These results confirm the successful transformation of the plasmids into yeast. No bands were observed in the negative control.

Analysis of surface-expressed target protein. Following successful transformation of the recombinant constructs, display of the recombinant Aga2–C-myc–EGFP–G4S–C1ND construct was examined. A colony of *S. cerevisiae* transformants was cultivated in SD–CAA liquid medium for 72 h at 30°C under orbital agitation (200 rpm). Following centrifugation, harvested cells were suspended in the appropriate lysis buffer. DTT was used; the treatment cleaved the disulfide linkages connecting Aga1 and Aga2, thereby releasing the Aga2–C-myc–EGFP–G4S–C1ND protein. As outlined in the Methods, lysates were examined using

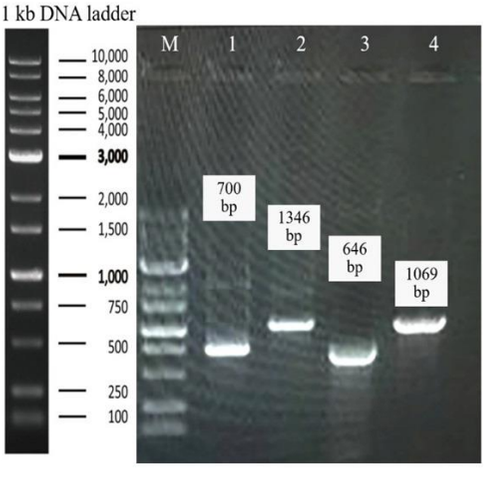

Fig. 2. PCR analysis of yeast transformants. Lanes 1 and 2 show the amplification of 700 bp and 1,346 bp fragments from pYES2-Tef1-display-GFP-C1ND using primers GFP-F/GFP-R and AGA2-F/C1ND-R, respectively. Lanes 3 and 4 show the PCR products of 646 bp and 1,069 bp from pYES2-Tef1-display-C1ND using primers AGA2-F/C1ND-R and TEF1-F/C1ND-R, respectively.

SDS–PAGE followed by Western blotting. Fig. 3 illustrates distinct protein bands (27, 24, and 50 kDa) representing *S. cerevisiae* cells expressing the GFP–C1ND construct. The 24 kDa band corresponds to the Aga2-C1ND fusion protein. These bands correspond to the Aga2–C-myc–G4S–C1ND and Aga2–C-myc–EGFP–G4S–C1ND recombinant proteins, confirming successful C1ND expression in *S. cerevisiae*. The 27 kDa band corresponds to the EGFP tag, which may have been cleaved during cell lysis. Blots in panels A and B were developed using ECL and DAB staining, respectively. In all blots, "C-" indicates non-transformed lysate. The positive control (lane 4, panel B, left image) expresses the intact C1ND fragment, displaying a band at 12 kDa. The positive control in panel B, right image (lane 2), corresponds to an irrelevant His-tagged protein.

Microscopic analysis of yeast-displayed C1ND fusion construct and C1ND-HopQ interaction. Confocal microscopy was utilized for validating protein display on the yeast cell surface of Aga2-EGFP-G4S-C1ND fusion proteins in *S. cerevisiae*. Yeast cells expressing the C1ND fusion protein were cultured for 72 hours in SD-CAA medium at 30°C with agitation at 200 rpm. Under the microscope, yeast cells expressing cells displaying Aga2–EGFP–G4S–C1ND on their surface emitted distinct green fluorescence. Additionally, the addition of PE-conjugated anti-GFP antibodies resulted in the Aga2-EGFP-G4S-C1ND recombinant protein localized to the cell surface appearing red, confirming surface expression of the C1ND fusion protein (Fig. 4). To analyze the interaction between yeast surface-displayed C1ND and HopQ, yeast cells expressing surface-displayed C1ND were incubated with recombinant HopQ-GFP protein and a recombinant *H. pylori* strain expressing GFP. The resulting interactions were visualized using confocal microscopy, as shown in Figs. 5 and 6. These figures demonstrate the interactions of both HopQ-GFP and the recombinant *H. pylori* strain with the target yeast cells. The negative control was made up of of *S. cerevisiae* harboring the empty pYES2 plasmid.

Specificity controls for C1ND-HopQ binding assays. To confirm the specificity of the observed interaction between surface-displayed C1ND and HopQ-GFP, several control experiments were performed. No green fluorescence was observed when yeast expressing AGA2-C1ND (without EGFP) was incubated with

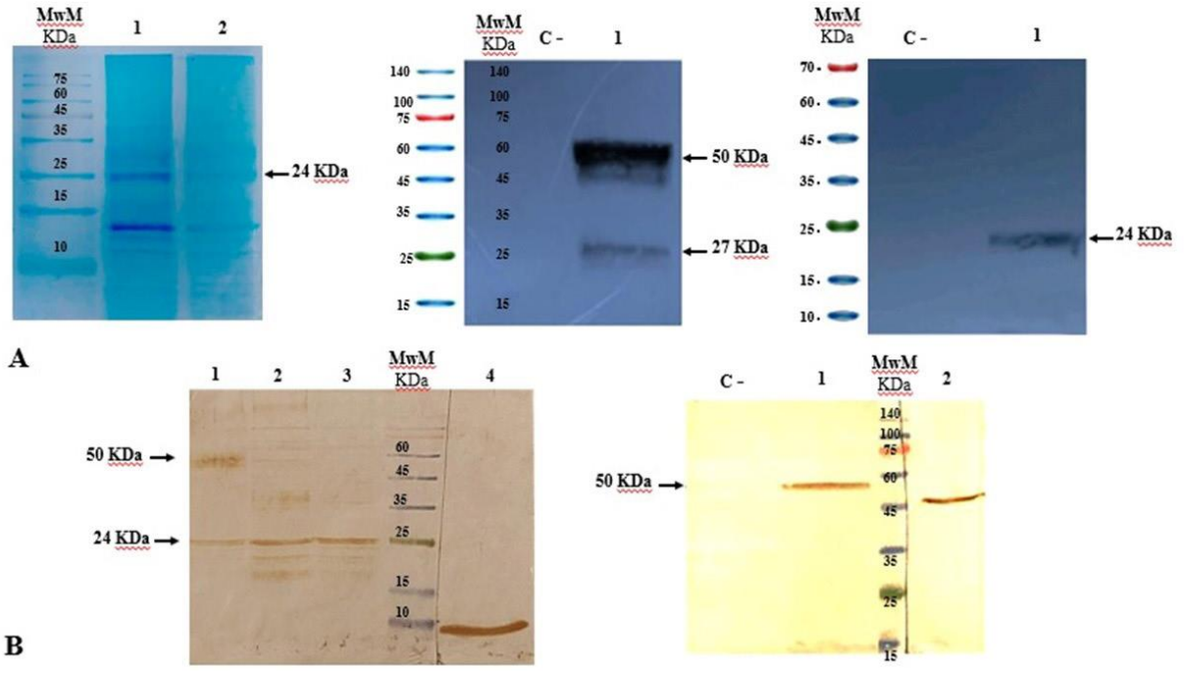

Fig. 3. SDS-PAGE and Western blot analyses. In panel A, the left image shows Coomassie Blue staining of *S. cerevisiae* expressing Aga2-C1ND (lanes 1 and 2). The middle blot shows two distinct bands at 50 kDa and 24 kDa detected using an HRP-conjugated anti-GFP antibody. Lane 1 corresponds to *S. cerevisiae* expressing the GFP-C1ND fusion construct. The presence of a 27 kDa band suggests cleavage of EGFP from its fusion partner. The right image shows signals detected by the anti-C1ND antibody for non-EGFP-tagged C1ND. The 24 kDa band corresponds to the Aga2-C1ND fusion protein. In panel B, the left image shows positive signals detected using the anti-C1ND antibody. Lane 1 shows the expression of the GFP-C1ND fusion protein, with bands at 24 kDa and 50 kDa. Lanes 2 and 3 represent strains expressing the Aga2-C1ND fusion protein, showing a band at 24 kDa. The positive control (lane 4) expresses the intact C1ND fragment, displaying a band at 12 kDa. The right image shows detection of the EGFP-C1ND fusion protein (50 kDa, lane 1) in a positive transformant using an HRP-conjugated anti-His-tag antibody. The positive control in this blot (lane 2) corresponds to an irrelevant His-tagged protein. In all blots, "C-" indicates non-transformed lysate. Blots in panels A and B were developed using ECL and DAB staining, respectively.

HOPQ-GFP, indicating no nonspecific binding. Furthermore, pre-incubation of AGA2-C1ND-expressing yeast with anti-C1ND antibody completely blocked the subsequent interaction with HOPQ-GFP, supporting the specific nature of the binding. Lastly, incubation of AGA2-C1ND-expressing yeast with AGA2-GFP also resulted in no detectable fluorescence signal, further confirming the specificity of the C1ND-HopQ interaction. These findings validate that the binding observed in our assays is specific and not due to non-specific protein-protein interactions (Fig. 7).

Flow cytometry analysis. The quantitative expression of the Aga2-EGFP-G4S-C1ND fusion protein in *S. cerevisiae* was quantified through flow cytometry. This process involved staining with phycoerythrin (PE)-labeled anti-GFP antibody to quantify the proportion of yeast cells expressing the C1ND-EGFP fusion protein on their surface. The surface-displayed proteins interacted with the PE-conjugated anti-GFP antibody, which enabled differentiation of recombinant proteins in yeast cells. Fig. 8, panel A, and Table 3 present the fluorescence intensity values compared to the negative control (*S. cerevisiae* harboring the empty pYES2 plasmid), while Fig. 8, panel B, and Table 4 compare the positive control with the negative control. Additionally, the mean fluorescence intensity (MFI) ratio was determined. Aga2–EGFP–G4S–C1ND transformants exhibited an MFI of 134, whereas negative controls showed 86.4. (Table 3). This difference was statistically significant between *S. cerevisiae* expressing Aga2-EGFP-G4S-C1ND and the negative control *S. cerevisiae* without plasmid ($P < 0.01$). In 100,000 yeast cells assessed for positive and

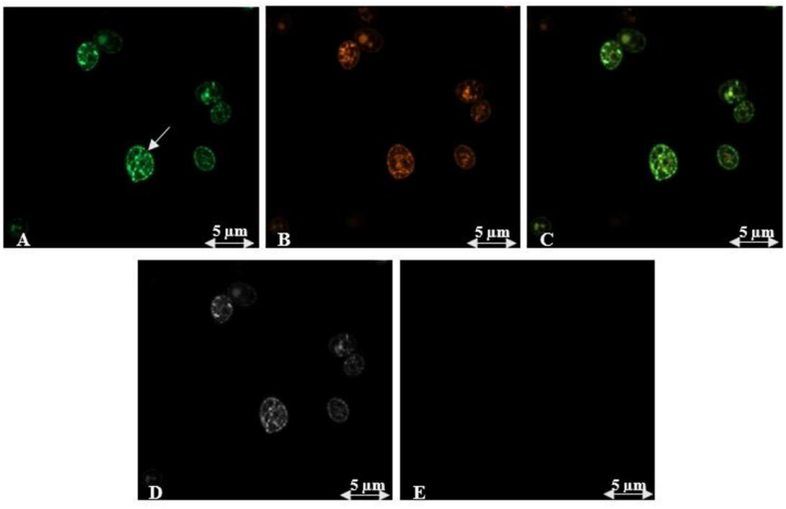

Fig. 4. Confocal microscopy images showing the surface expression of the Aga2-EGFP-G4S-C1ND fusion protein in *S. cerevisiae*, indicated by arrows. (A) Green fluorescence from the EGFP tag. (B) Red surface fluorescence of recombinant yeast cells stained with PE-conjugated anti-GFP antibody. (C) Merged image of panels A and B. (D) Brightfield image. (E) No fluorescence in the negative control. Scale bar: 5 µm

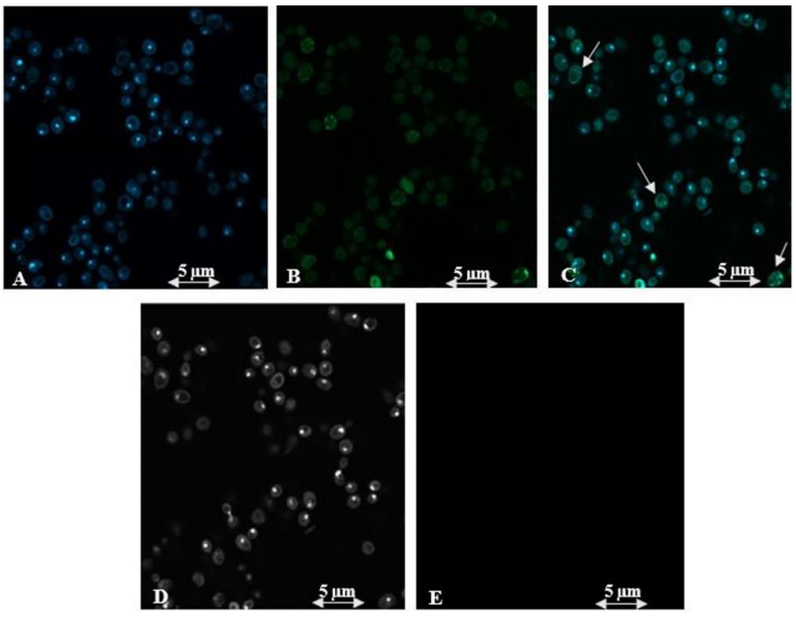

Fig. 5. Confocal microscopic visualization of the interaction between *S. cerevisiae* displaying C1ND on its surface and recombinant HopQ–GFP protein (arrows). (A) DAPI-stained image of *S. cerevisiae.* (B) GFP fluorescence of the same field. (C) Overlay of A and B. (D) Brightfield image of the negative-control cells. (E) Fluorescence image of the negative control. Scale bar = 5 µm.

negative samples, the expression rate of the pYES2-Tef1-display-C1ND construct was 27.9%, as calculated using FlowJo 7.6.1 software. *S. cerevisiae* harboring the empty pYES2 plasmid served as the negative control in flow cytometric assays. Flow cytometric analysis of *S. cerevisiae* is shown in Figs. 8 and 9.

Statistical analysis of mean fluorescence intensity (MFI) between groups. Comparison of *S. cerevisiae*-C1ND group with negative control (*S. cerevisiae* harboring empty pYES2):

Flow cytometric evaluation demonstrated that the average MFI of the *S. cerevisiae*–C1ND group (133.67

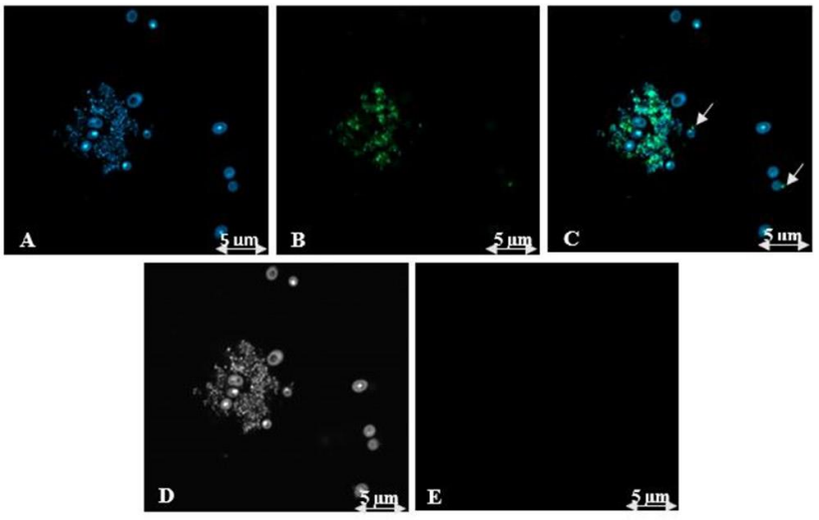

Fig. 6. Confocal microscopy analysis of the interaction between recombinant *S. cerevisiae* expressing surface-displayed C1ND and *H. pylori* expressing GFP. (A) *S. cerevisiae* interacting with *H. pylori*, captured using the DAPI filter. (B) *S. cerevisiae* and *H. pylori* observed under the GFP filter. (C) Merged image of panels A and B, with the interaction indicated by arrows. (D) Brightfield micrograph of the negative control *S. cerevisiae*. (E) Fluorescence micrograph of the negative control *S. cerevisiae*. Scale bar: 5 µm.

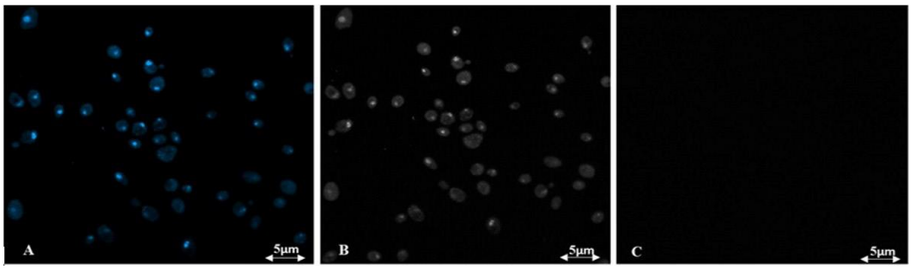

Fig. 7. Confocal imaging of the interaction between recombinant *S. cerevisiae* displaying surface C1ND and the fusion protein HopQ–GFP. Cells were analyzed after 72 h of growth in SD–CAA medium. To evaluate binding, anti-C1ND antibody was applied, followed by fixation with paraformaldehyde and nuclear stained by means of DAPI (4′,6-diamidino-2-phenylindole). Image A: DAPI channel of recombinant *S. cerevisiae* showing surface-expressed C1ND. Image B: GFP channel of the same field showing no green signal, indicating absence of interaction between AGA2–C1ND and HopQ–GFP. Image C: Negative-control cells harboring the empty pYES2 vector. Scale = 5 µm.

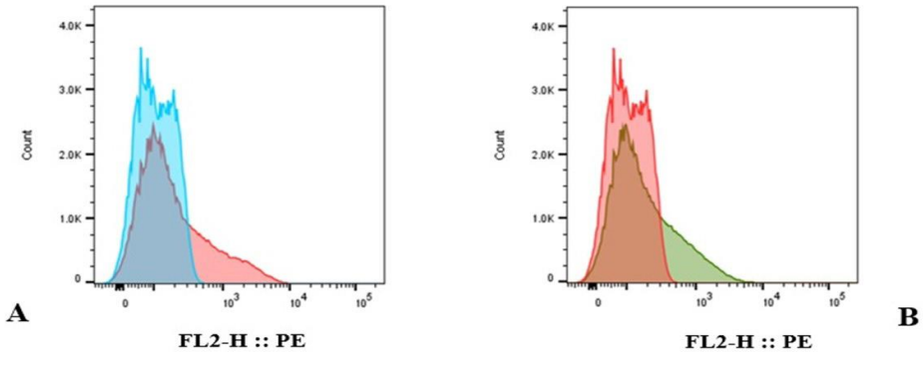

Fig. 8. Flow cytometric analysis of *S. cerevisiae* cells expressing surface-displayed Aga2-EGFP-G4S-C1ND fusion protein. (A) Histogram of *S. cerevisiae* cells expressing the C1ND fusion protein. (B) Histogram of *S. boulardii* cells expressing Aga2-EGFP-G4S-PLI1 fusion protein, used solely as a positive technical control derived from an unrelated project and not part of the main objectives of this study.

Table 3. Fluorescence intensity values compared to the negative control (*Saccharomyces cerevisiae*)

Subset name	Mean FL2-H (MFI)
Negative control (*S. cerevisiae* harboring empty pYES2 plasmid)	86.4
S. cerevisiae expressing Aga2-EGFP-G4S-C1ND	134

Table 4. Comparison of fluorescence intensity values between positive and negative control samples

Subset name	Mean FL2-H (MFI)
Negative Control (*S. cerevisiae* harboring empty pYES2 plasmid)	88.5
S. boulardii expressing PLI1	117

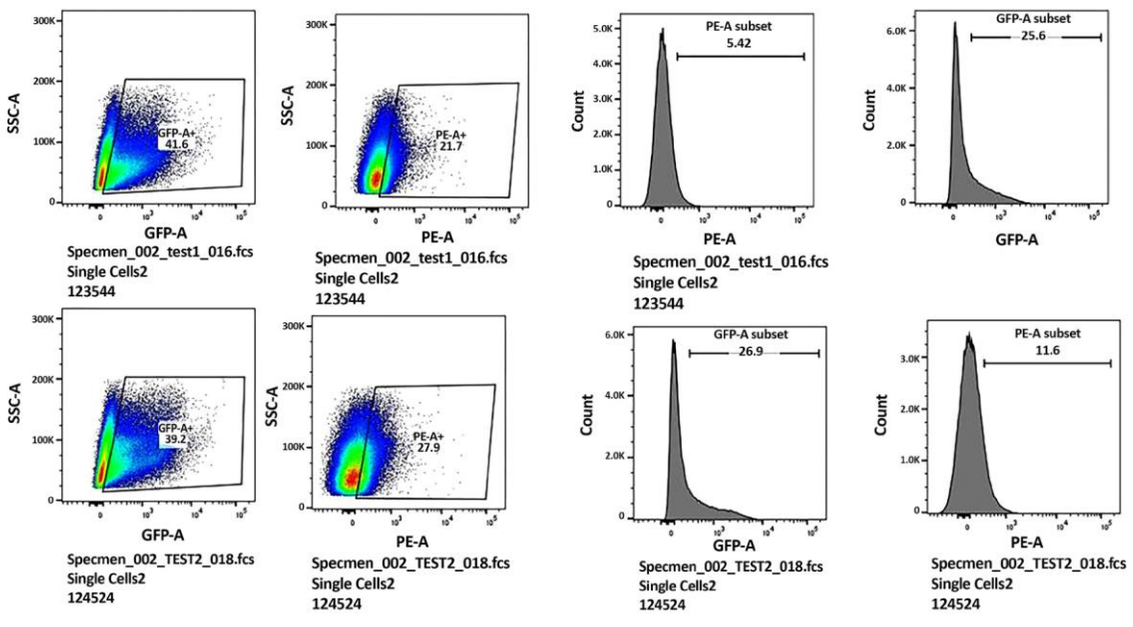

Fig. 9. Flow cytometry 4-quadrant diagram. The upper panel corresponds to *S. boulardii* cells expressing Aga2-EGFP-G4S-PLI1 fusion protein. The lower panel corresponds to *S. cerevisiae* cells expressing surface-displayed Aga2-EGFP-G4S-C1ND fusion protein, used solely as a positive technical control derived from an unrelated project and not part of the main objectives of this study.

± 0.58) was higher than that of the negative control (107.67 ± 1.15). Statistical analysis using Welch's t-test confirmed that a measurable distinction was detected between these experimental groups (t = 6.05, P = 0.00006). The 95% confidence interval for the mean difference ranged from 19.8 to 33.1.

Comparison of *S. boulardii*-PLI1 group with negative control (*S. cerevisiae* harboring empty pYES2):

The mean MFI in the *S. boulardii*-PLI1 group was 116.33 ± 1.15, compared to 107.67 ± 1.15 in the negative control group. According to Welch's t-test, the variation between the two groups reached statistical significance (t = 4.55, P = 0.00078). The 95% confidence interval for the difference in means was 4.2–13.4, confirming the significant difference, as illustrated graphically in Fig. 10.

DISCUSSION

Protein display technology has facilitated the directed evolution of protein properties, enabling improvements in binding affinity, activity, and stability (36). Yeast cells are well-suited for expressing com-

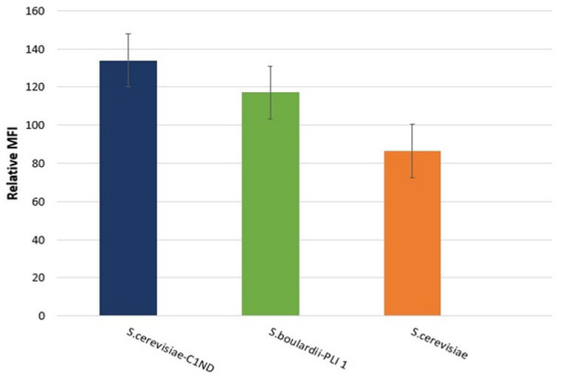

Fig. 10. Graph showing the ratio of MFI of *S. cerevisiae* expressing C1ND compared to the negative control (*S. cerevisiae* harboring empty pYES2 plasmid) and showing the ratio of MFI of *S. bulardii* expressing PLI1 compared to the negative control (*S. cerevisiae* harboring empty pYES2 plasmid), with a statistically significant difference ($P < 0.01$).

plex eukaryotic proteins due to their protein secretion pathway and post-translational modification capabilities (37). Yeast surface display serves as an efficient platform for analyzing protein–protein interactions and optimizing binding affinity (27, 38). This technology has been instrumental in various studies. For example, it has been used to display Tau protein, which is critical for neurodegenerative research, enabling investigations into protein interaction patterns and structural changes with significant potential for detecting neurodegenerative disease markers (39). Additionally, the surface expression of HIV envelope glycoproteins has advanced immunotherapy research by enhancing immune responses against the virus (40). Incorporating GPCRs into yeast display systems represents a significant advancement for viral detection assays, offering potential applications in diagnosing and treating viral infections, particularly relevant during viral outbreaks such as the recent COVID-19 pandemic (41). In another innovative approach, Autonomous Hypermutation Yeast Surface Display (AHEAD) enabled the accelerated generation of high-affinity nanobodies for various targets, demonstrating its efficiency in antibody development (42). Beyond antibodies, yeast surface display has shown promise in functionalizing proteins such as CD81, expanding its potential applications in drug delivery via extracellular vehicles (EVs) (43). In a recent study by Nayebhashemi et al. (32), live probiotic yeast was engineered to express Pancreatic Lipase Inhibitor (PLI) peptides using a yeast surface display system. This approach demonstrated the potential of recombinant probiotic yeasts for anti-obesity interventions, with oral administration leading to significant weight loss and reduced serum lipid levels in a mouse model. This research highlights the diverse applications of yeast surface display in drug discovery and underscores the potential of intact live yeast as a promising therapeutic modality. In the present study, we successfully expressed C1ND by applying yeast surface display to explore its interaction with the *H. pylori* HopQ protein.

This research introduces an innovative yeast surface display model in which the N-terminal domain of CEACAM1 (C1ND) is presented on the surface of *S. cerevisiae* to analyze its molecular interaction with *H. pylori* HopQ. Previous studies have not used surface-displayed C1ND to investigate the CEACAM1-HopQ interaction in *H. pylori*, representing a novel approach in our work. This innovation establishes a proof-of-concept platform that could be further developed for screening potential inhibitors targeting this interaction.

H. pylori is a well-known bacterium that colonizes the gastric mucosa and is associated with various diseases, including gastritis, peptic ulcers, and gastric cancer (44).

Numerous studies have aimed to prevent *H. pylori* infection by disrupting its attachment to gastric epithelial cells. A key focus of these studies is the interaction between *H. pylori* and gastric epithelial receptors, especially the HopQ–CEACAM binding mechanism. The HopQ–CEACAM interaction, which promotes *H. pylori* virulence through CagA translocation into host epithelial cells, has recently attracted considerable attention. For example, experimental data show that deletion of both HopQ and CEACAM receptors almost completely abolishes CagA translocation, highlighting the critical role of this interaction in pathogenicity (9). CEACAM1, CEACAM3, CEACAM5, and CEACAM6 were recognized as new *H. pylori* receptors, with binding mediated through their IgV-like N-terminal domains. These results highlight the critical role of HopQ–CEACAM binding in the translocation of CagA (16). Javaheri et al. (2016) revealed that HopQ binds CEACAM1, CEACAM3, CEACAM5, and CEACAM6 in a glycan-independent manner, offering possible therapeutic avenues against *H. pylori* infection. Structural studies pinpointed a β-hairpin motif within the extracellular 3+4 helix bundle of HopQ as crucial for

CEACAM recognition (23). Additionally, they elucidated the structures of multiple HopQ-CEACAM complexes, as well as CEACAM in monomeric and dimeric assemblies, suggesting that HopQ employs simultaneous folding and binding mechanisms to interact with the dimerization interface of CEACAM for recognition. They also detailed the molecular mechanisms of CEACAM and HopQ interactions. Understanding these molecular interactions may pave the way for developing novel therapeutic strategies, including inhibitors of oncoprotein translocation and *H. pylori*-specific antimicrobial agents (17).

Crystal structures of HopQ isoforms I and II complexed with C1ND have revealed detailed insights into *H. pylori*–CEACAM receptor interactions. Each HopQ variant recognizes distinct structural motifs within C1ND that are essential for CEACAM binding. Using small-angle X-ray scattering (SAXS), the authors showed that HopQ alone promotes C1ND monomerization, influencing cell adhesion and CEACAM-dependent signaling via conformational rearrangements in *H. pylori* (24).

In our study, a yeast platform was implemented for the surface expression of C1ND in *S. cerevisiae*. In this system, the strong constitutive Tef1 promoter drives the expression of Aga1 and Aga2 proteins, which are essential for the proper localization and consistent surface display of C1ND. Expression of the fusion protein was validated using immunofluorescence, confocal microscopy, and Western blot techniques. Confocal microscopy further revealed specific binding of both GFP-labeled HopQ and *H. pylori* expressing GFP to the surface of yeast cells displaying C1ND, with no binding observed in the negative control yeast. This approach is consistent with the work of Wu et al. (2017) (45), who engineered an LPETG-EGFP fusion protein for yeast surface display, significantly reducing costs associated with fluorescence resonance energy transfer substrates commonly used in high-throughput sortase A inhibitor screening. It should be noted that the current study does not involve the identification or testing of inhibitors; instead, it establishes a proof-of-concept system for studying the HopQ-CEACAM1 interaction.

This study has several important limitations. First, we did not assess the biological functionality of the displayed C1ND domain, such as its ability to mediate downstream signaling or internalization upon binding HopQ. Second, quantitative binding analyses, including surface plasmon resonance (SPR) or bio-layer interferometry (BLI), were not performed to determine the precise binding affinity and kinetics of the HopQ-CEACAM1 interaction. Third, although initial specificity tests were conducted, additional controls, such as mutant HopQ proteins or irrelevant CEACAM isoforms (e.g., CEACAM8), are needed to further validate the specificity of the observed interactions.

CONCLUSION

In conclusion, this study successfully demonstrated the surface expression of the N-terminal IgV-like domain of CEACAM1 (C1ND) on *Saccharomyces cerevisiae* using yeast surface display technology, and showed its specific binding to the *H. pylori* adhesin HopQ. Our results confirm the feasibility of this platform as a preliminary validation system for studying the HopQ-CEACAM1 engagement. This platform could be utilized in future research to identify or screen potential inhibitors that block this critical host-pathogen interaction, which may ultimately contribute to strategies aimed at preventing *H. pylori* adhesion and associated pathogenesis.

ACKNOWLEDGEMENTS

The authors express their gratitude for the technical assistance provided by Islamic Azad University, North Tehran Branch, Iran.

REFERENCES

1. Hooi JK, Lai WY, Ng WK, Suen MM, Underwood FE, Tanyingoh D, et al. Global prevalence of *Helicobacter pylori* infection: systematic review and meta-analysis. *Gastroenterology* 2017; 153: 420-429.
2. Zamani M, Ebrahimtabar F, Zamani V, Miller W, Alizadeh-Navaei R, Shokri-Shirvani J, et al. Systematic review with meta-analysis: the worldwide prevalence of *Helicobacter pylori* infection. *Aliment Pharmacol Ther* 2018; 47: 868-876.
3. Salama NR, Hartung ML, Müller A. Life in the human stomach: persistence strategies of the bacterial pathogen *Helicobacter pylori*. *Nat Rev Microbiol* 2013; 11: 385-399.

4. Wroblewski LE, Peek Jr RM, Wilson KT. *Helicobacter pylori* and gastric cancer: factors that modulate disease risk. *Clin Microbiol Rev* 2010; 23: 713-739.
5. Gur C, Maalouf N, Gerhard M, Singer BB, Emgård J, Temper V, et al. The *Helicobacter pylori* HopQ outermembrane protein inhibits immune cell activities. *Oncoimmunology* 2019; 8(4): e1553487.
6. Hatakeyama M. *Helicobacter pylori* oncoprotein CagA and bacterial EPIYA effector family. *Seikagaku* 2014; 86: 744-754.
7. Backert S, Moese S, Selbach M, Brinkmann V, Meyer TF. Phosphorylation of tyrosine 972 of the *Helicobacter pylori* CagA protein is essential for induction of a scattering phenotype in gastric epithelial cells. *Mol Microbiol* 2001; 42: 631-644.
8. Backert S, Tegtmeyer N, Selbach M. The versatility of *Helicobacter pylori* CagA effector protein functions: The master key hypothesis. *Helicobacter* 2010; 15: 163-176.
9. Zhao Q, Busch B, Jiménez-Soto LF, Ishikawa-Ankerhold H, Massberg S, Terradot L, et al. Integrin but not CEACAM receptors are dispensable for *Helicobacter pylori* CagA translocation. *PLoS Pathog* 2018; 14(10): e1007359.
10. Hatakeyama M, Higashi H. *Helicobacter pylori* CagA: a new paradigm for bacterial carcinogenesis. *Cancer Sci* 2005; 96: 835-843.
11. Matsuo Y, Kido Y, Yamaoka Y. *Helicobacter pylori* outer membrane protein-related pathogenesis. *Toxins (Basel)* 2017; 9: 101.
12. Nguyen QA, Schmitt L, Mejías-Luque R, Gerhard M. Effects of *Helicobacter pylori* adhesin HopQ binding to CEACAM receptors in the human stomach. *Front Immunol* 2023; 14: 1113478.
13. Kalali B, Mejías-Luque R, Javaheri A, Gerhard M. *H. pylori* virulence factors: influence on immune system and pathology. *Mediators Inflamm* 2014; 2014: 426309.
14. Ansari S, Yamaoka Y. *Helicobacter pylori* virulence factors exploiting gastric colonization and its pathogenicity. *Toxins (Basel)* 2019; 11: 677.
15. Cao P, Cover TL. Two different families of hopQ alleles in *Helicobacter pylori*. *J Clin Microbiol* 2002; 40: 4504-4511.
16. Königer V, Holsten L, Harrison U, Busch B, Loell E, Zhao Q, et al. Erratum: *Helicobacter pylori* exploits human CEACAMs via HopQ for adherence and translocation of CagA. *Nat Microbiol* 2016; 2: 16233.
17. Bonsor DA, Zhao Q, Schmidinger B, Weiss E, Wang J, Deredge D, et al. The *Helicobacter pylori* adhesin protein HopQ exploits the dimer interface of human CEACAMs to facilitate translocation of the oncoprotein CagA. *EMBO J* 2018; 37(13): e98664.
18. Zhuo Y, Yang J-Y, Moremen KW, Prestegard JH. Correction: Glycosylation alters dimerization properties of a cell-surface signaling protein, carcinoembryonic antigen-related cell adhesion molecule 1 (CEACAM1). *J Biol Chem* 2020; 295: 3748.
19. Ru G-Q, Han Y, Wang W, Chen Y, Wang H-J, Xu W-J, et al. CEACAM6 is a prognostic biomarker and potential therapeutic target for gastric carcinoma. *Oncotarget* 2017; 8: 83673-83683.
20. Hall C, Clarke L, Pal A, Buchwald P, Eglinton T, Wakeman C, et al. A review of the role of carcinoembryonic antigen in clinical practice. *Ann Coloproctol* 2019; 35: 294-305.
21. Najjar SM. Regulation of insulin action by CEACAM1. *Trends Endocrinol Metab* 2002; 13: 240-245.
22. Beauchemin N, Arabzadeh A. Carcinoembryonic antigen-related cell adhesion molecules (CEACAMs) in cancer progression and metastasis. *Cancer Metastasis Rev* 2013; 32: 643-671.
23. Javaheri A, Kruse T, Moonens K, Mejías-Luque R, Debraekeleer A, Asche CI, et al. *Helicobacter pylori* adhesin HopQ engages in a virulence-enhancing interaction with human CEACAMs. *Nat Microbiol* 2016; 2: 16189.
24. Moonens K, Hamway Y, Neddermann M, Reschke M, Tegtmeyer N, Kruse T, et al. *Helicobacter pylori* adhesin HopQ disrupts trans dimerization in human CEACAM s. *EMBO J* 2018; 37(13): e98665.
25. Huang Y-H, Zhu C, Kondo Y, Anderson AC, Gandhi A, Russell A, et al. CEACAM1 regulates TIM-3-mediated tolerance and exhaustion. *Nature* 2015; 517: 386-390.
26. Lee SY, Choi JH, Xu Z. Microbial cell-surface display. *Trends Biotechnol* 2003; 21: 45-52.
27. Löfblom J. Bacterial display in combinatorial protein engineering. *Biotechnol J* 2011; 6: 1115-1129.
28. Ueda M, Tanaka A. Cell surface engineering of yeast: construction of arming yeast with biocatalyst. *J Biosci Bioeng* 2000; 90: 125-136.
29. Kondo A, Ueda M. Yeast cell-surface display—applications of molecular display. *Appl Microbiol Biotechnol* 2004; 64: 28-40.
30. Lopez-Morales J, Vanella R, Appelt EA, Whillock S, Paulk AM, Shusta EV, et al. Protein engineering and High-Throughput screening by yeast surface display: survey of current methods. *Small Sci* 2023; 3: 2300095.
31. Yang F, Cao M, Jin Y, Yang X, Tian S. Construction of a novel a-agglutinin expression system on the surface of wild-type *Saccharomyces cerevisiae* Y5 and genetic immobilization of β-glucosidase1. *BioEnergy Res* 2013; 6: 1205-1211.
32. Nayebhashemi M, Enayati S, Zahmatkesh M, Madanchi H, Saberi S, Mostafavi E, et al. Surface display of pancreatic lipase inhibitor peptides by engineered *Saccharomyces boulardii*: Potential as an anti-obesity probiotic. *J Funct Foods* 2023; 102: 105458.
33. Benatuil L, Perez JM, Belk J, Hsieh C-M. An improved

yeast transformation method for the generation of very large human antibody libraries. *Protein Eng Des Sel* 2010; 23: 155-159.
34. Uchański T, Zögg T, Yin J, Yuan D, Wohlkönig A, Fischer B, et al. An improved yeast surface display platform for the screening of nanobody immune libraries. *Sci Rep* 2019; 9: 382.
35. Sing CN, Yang EJ, Higuchi-Sanabria R, Pon LA, Boldogh IR, Swayne TC. Imaging the actin cytoskeleton in fixed budding yeast cells. *Methods Mol Biol* 2022; 2364: 81-100.
36. Prole DL, Chinnery PF, Jones NS. Visualizing, quantifying, and manipulating mitochondrial DNA in vivo. *J Biol Chem* 2020; 295: 17588-17601.
37. Teymennet-Ramírez KV, Martínez-Morales F, Trejo-Hernández MR. Yeast surface display system: Strategies for improvement and biotechnological applications. *Front Bioeng Biotechnol* 2022; 9: 794742.
38. Tanaka T, Yamada R, Ogino C, Kondo A. Recent developments in yeast cell surface display toward extended applications in biotechnology. *Appl Microbiol Biotechnol* 2012; 95: 577-591.
39. Wang S, Cho YK. Yeast surface display of full-length human microtubule-associated protein tau. *Biotechnol Prog* 2020; 36(1): e2920.
40. Mathew E, Zhu H, Connelly SM, Sullivan MA, Brewer MG, Piepenbrink MS, et al. Display of the HIV envelope protein at the yeast cell surface for immunogen development. *PLoS One* 2018; 13(10): e0205756.
41. Maneira C, Bermejo PM, Pereira GAG, de Mello FDSB. Exploring G protein-coupled receptors and yeast surface display strategies for viral detection in baker's yeast: SARS-CoV-2 as a case study. *FEMS Yeast Res* 2021; 21: foab004.
42. Wellner A, McMahon C, Gilman MS, Clements JR, Clark S, Nguyen KM, et al. Rapid generation of potent antibodies by autonomous hypermutation in yeast. *Nat Chem Biol* 2021; 17: 1057-1064.
43. Vogt S, Stadlmayr G, Stadlbauer K, Stracke F, Bobbili MR, Grillari J, et al. Construction of Yeast Display Libraries for Selection of Antigen-Binding Variants of Large Extracellular Loop of CD81, a Major Surface Marker Protein of Extracellular Vesicles. *Methods Mol Biol* 2022; 2491: 561-592.
44. Peek RM Jr, Blaser MJ. *Helicobacter pylori* and gastrointestinal tract adenocarcinomas. *Nat Rev Cancer* 2002; 2: 28-37.
45. Wu L, Li H, Tang T. A novel yeast surface display method for large-scale screen inhibitors of sortase A. *Bioengineering (Basel)* 2017; 4: 6.